BASIC STUDY ON HIGH-GRADIENT ACCELERATING STRUCTURES AT KEK / NEXTEF

Tetsuo Abe*, Yoshio Arakida, Toshiyasu Higo, Shuji Matsumoto, Toshikazu Takatomi,
KEK, Tsukuba, Ibaraki 305-0801, Japan

Abstract

So far, we have developed X-band high-gradient accelerating structures of prototypes for normal-conducting linear colliers in a comprehensive way, establishing a full production process of fabrication and test. On the other hand, focusing on the fact that we do not know both the high-gradient limit of performance and breakdown trigger mechanism on the normal-conducting RF acceleration, we have been preparing a new test stand for a fresh basic study on vacuum breakdown, where we use compact test structures with an RF field concentrated in a single test cell.

In this paper, we report the status of the new test stand called "Shield-B" together with a list of test structures ready for high-gradient test or under fabrication.

INTRODUCTION

X-band (11.4 GHz) normal-conducting RF acceleration technology can be applied to high-gradient accelerators, such as compact linear colliders and medical linacs. Based on the development results and experiences through the NLC/GLC projects (aiming at an operational gradient of 65 MV/m) [1], high-gradient accelerating structures with higher-order-mode (HOM) damped structure (hereinafter simply referred to as "damped structure") have been developed, aiming at an operational gradient of 100 MV/m [2]. We also have been establishing a full production process of fabrication and test of prototype structures, including

1. Machining of components, such as disks and waveguides,
2. Cleaning and surface process, such as chemical polishing of disks,
3. Diffusion bonding of disks,
4. Assembly,
5. Pretest low-power RF measurement,
6. Vacuum baking,
7. High-gradient test,
8. Posttest low-power RF measurement, and
9. Postmortem by microscopy.

One of the recent significant achievements is a high-gradient test result of a multi-cell prototype structure for CLIC [3], which meets requirements of CLIC: an accelerating gradient (E_{acc}) of 100 MV/m, an RF pulse width around 200 ns, a repetition rate of 50 Hz, and a breakdown rate (BDR) lower than 3×10^{-7} /m/pulse although this has no damped structure (undamped structure) [4]. The latest prototype structure for CLIC has a HOM heavily damped structure with waveguides (HOM waveguides), which has about two orders of magnitude higher BDR than that of the corresponding undamped one [5]. Although it has been found that such large BDR difference is related to the large surface current around the HOM waveguides [10, 11], we do not yet fully understand the real reason, and in addition, we do not know the real cause of breakdown (breakdown trigger mechanism); these two facts motivate us to perform further basic study on breakdown characteristics of the structures.

In parallel with the above-mentioned comprehensive development of multi-cell prototypes, we have been preparing a test stand focused on basic study on vacuum breakdown, in collaboration with the high-gradient accelerating-structure development teams at CERN and SLAC, because such comprehensive development is cost and time consuming. Here, we use compact test cavities with an RF field concentrated in a single test cell coupled with an upstream coupling cell and a downstream end cell. This is a minimum structure keeping a realistic RF field for acceleration in the test cell, and easy to make and test. In this study, we refer to this three-cavity structure as "single-cell structure." This type of testing method is originated from [6].

In this paper, we report the status of our new test stand called "Shield-B" at KEK / Nextef for implementing the above-mentioned agile experimental research, followed by showing accelerating structures to be tested at the test stand in the near future.

TEST STAND

Figure 1 shows our X-band test facility: Nextef, which consists of two radiation shields of Shield-A and Shield-B. In Shield-A, we perform high-gradient tests of multi-cell prototypes, while in Shield-B, high-gradient tests for basic study using single-cell structures will be performed. As shown in Fig. 1, the X-band klystron for Shied-B is not located in the same room as Shield-B, so that we have constructed a 30 m-long high-power RF transmission line (power line), as shown with a red dashed line in Fig. 1. The major part of the power line is a low-loss line consisting of a circular waveguide (WC40) for TE_{01} mode. The inside of the power line has been evacuated into ultrahigh vacuum.

Figure 2 shows the current status of Shield-B, where the power line is terminated by a dummy load. We have been performing RF conditioning of the power line, as shown in Fig. 3, reaching 6.8 MW of input RF power as of July 28, 2015. The current target is 10 MW, which corresponds to 100 MW/m at the test cell of a single-cell structure.

TEST STRUCTURES

All of the test structures shown in this paper:

* tetsuo.abe@kek.jp

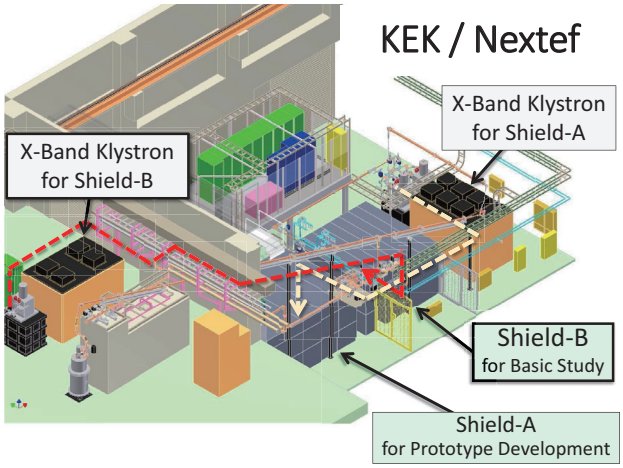

Figure 1: X-band test facility: Nextef. The red (light yellow) dashed line indicates a power line for Shield-B (Shield-A).

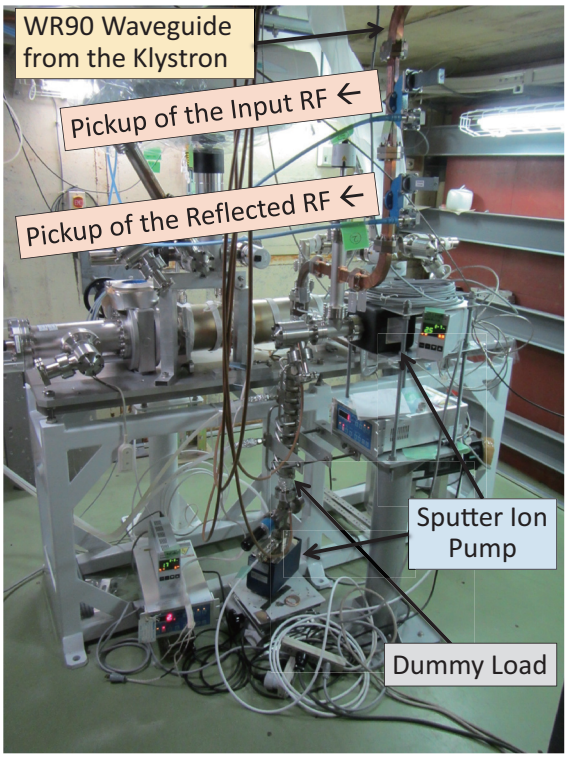

Figure 2: Photograph of the inside of Shield-B as of July, 2015.

- Consist of three cells of a coupling cell, an end cell, and a test cell in-between,
- Made of high-purity oxygen-free copper satisfying C10100, where unless otherwise specified, the grain size of the copper material is of the order of 0.1 mm after fabrication, and
- Are used to excite π-mode like standing wave as an accelerating mode.

We have various test structures to be high-gradient tested and compared, as classified and summarized in Tab. 1,

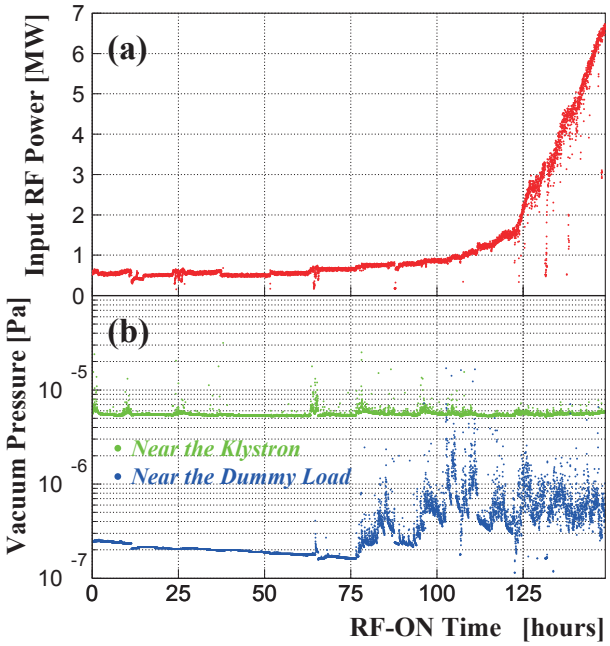

Figure 3: Status of RF conditioning of the power line until July 28, 2015, where only the data with non-zero input RF power are plotted here. (a) RF power input to the dummy load. (b) Vacuum pressure inside the power line.

which will be explained in detail in the following subsections.

Undamped Structures

Although our ultimate goal is to have an damped structure with a sufficiently-low BDR at E_{acc} = 100 MV/m or higher, undamped structures are useful to understand basic characteristics of test structures on geometries, materials, machining, cleaning, and other characteristics not related to the damped structure. What is also important is that an undamped structure, made of usual material, machined and fabricated in a usual way for prototype structures can be a "reference" in BDR measurements. Hereinafter referred to this cavity as "standard cavity."

Standard cavity Although there are various geometries of undamped single-cell structures tested so far [7], we have chosen a geometry with an iris aperture radius of a = 3.75 mm and iris thickness of t = 2.6 mm as a "standard" geometry in this study. Figure 4a shows its solid model. This geometry can be machined only by turning with an arithmetical mean roughness (R_a) of 0.03 to 0.1 μm for the inner surface, where the skin depth of copper is $\approx$ 0.5 μm at 11.4 GHz. Figure 4b and 4c show RF field of the accelerating mode (π-mode like). Frequency of the coupling and end cells are slightly detuned so that the field strength in the test cell is almost double of those in the coupling and end cells as shown in Fig. 5.

Table 1: Classification of the materials, methods, and structures to be high-gradient tested at Shield-B. Items described in parentheses indicate future options.

Structure	Undamped Disk-type	Damped with HOM waveguides Disk-type	Damped with HOM waveguides Quadrant-type	Choke-mode damped Disk-type
Grain size of copper material	≈ 0.1 mm or 5 to 50 mm (6N)	≈ 0.1 mm	≈ 0.1 mm	≈ 0.1 mm
Machining method for disks or quadrants	Turning only or Milling only	Turning + Milling	Milling only	Turning only
Surface finishing	Chemical polishing	Chemical polishing	None (Advanced polishing)	None
Bonding method for disks or quadrants	Diffusion bonding	Diffusion bonding or Brazing	EBW (or Brazing)	Diffusion bonding

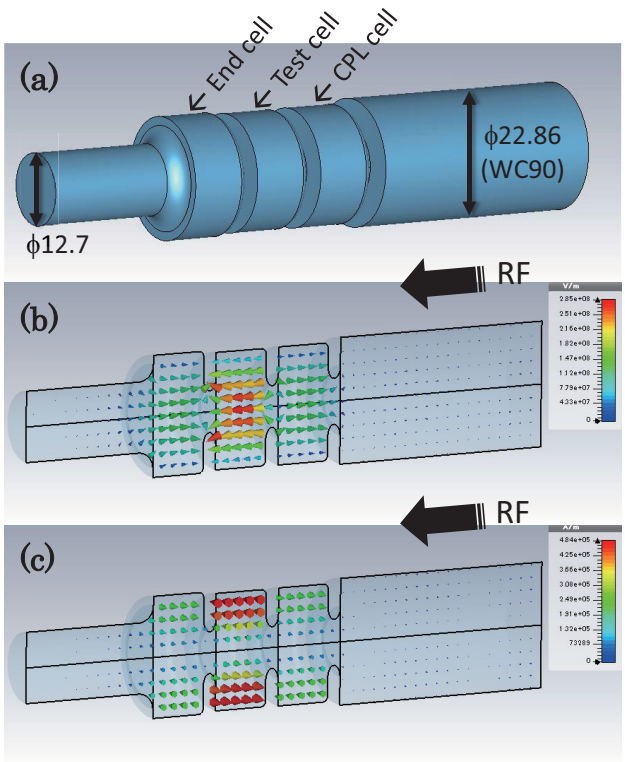

Figure 4: RF simulation for the standard cavity. (a) Solid model (vacuum region). (b) Electric and (c) magnetic field of the accelerating mode (π-mode like). CPL means coupling.

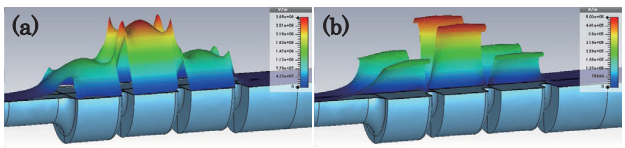

Figure 5: Magnitude of the RF field of the accelerating mode shown as a height of the carpet in linear scale. Input RF wave comes from the right. (a) Electric field strength. (b) Magnetic field strength.

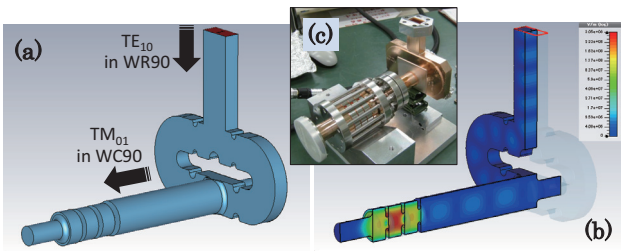

Figure 6: Standard cavity mounted with the mode converter (TE_{10} in the rectangular waveguide (WR90) to TM_{01} in the circular waveguide (WC90)). (a) Solid model of the vacuum region. (b) Snapshot of the electric-field strength shown in log scale. (c) Photograph of a corresponding real setup, including the standard cavity and the mode converter.

Since RF power is delivered to a test cavity as a TE_{10} mode in the rectangular waveguide (WR90), we use a reusable mode converter to launch TM_{01} mode in a circular waveguide (WC90) [8] located close to the test structure. Such mode converter can be used for any other test cavities. Figure 6 shows a conceptual diagram including the mode converter.

Made of large-grain copper Grain boundary is one of the most significant crystal defects. There is speculation that BDR has some correlation with grain boundaries because surface damage by electro-migration [9] is relatively large at grain boundaries. We have been making undamped test cavities with the same geometry as that of the standard cavity with a grain size of 5 to 50 mm from six nines copper.

Machined by milling only Damped structures with HOM waveguides cannot be machined without milling. Surface roughness (damage) by milling is large (deep) in case of milling compared with surface by turning, which is guess to have any effect on BDR. We have been making undamped test cavities with the same geometry as that

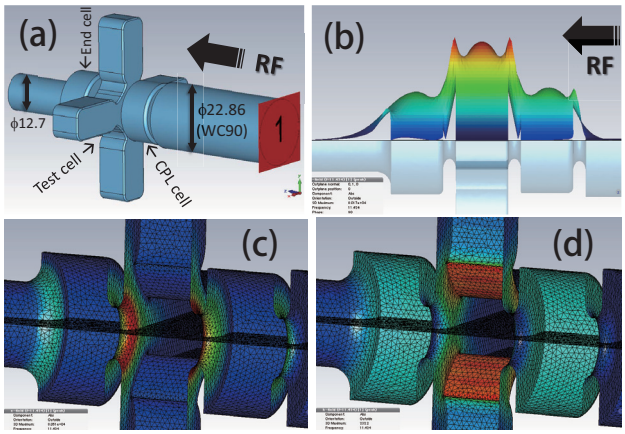

Figure 7: Test cavity with HOM waveguides. For the solid model shown in (a), simulation results on (b) the electric-field strength, (c) surface electric field, and (d) surface magnetic field of the the accelerating mode are shown. Also shown in (c) and (d) is curved tetrahedral meshing used in this RF simulation. CPL means coupling.

of the standard cavity, machined by milling only (without turning).

Damped Structures with HOM Waveguides

For high-energy applications, damped structures are often required. HOM damping with waveguides is a simple and promising way although surface magnetic field, or surface current, is enhanced around the HOM waveguides, and resultant BDR is orders of magnitude higher than that of a corresponding undamped structure, as shown in the recent high-gradient tests [5]. We study effects of such damped structure with different fabrication methods for comparison, where the coupling and end cells are basically have the same geometry as those of the standard cavity except for the coupling iris.

Figure 7a is the solid model, where the design of the test cell is based on the optimized structure for CLIC called "TD24R05" [3, 5]. Figure 7b shows magnitude of the electric field, and Fig. 7c (7d) shows the surface electric (magnetic) field strength.

Consisting of disks (disk-type) diffusion-bonded We have made disks of the damped test cell, which will be diffusion-bonded with disks of the coupling and end cells in the standard method applied to multi-cell prototype structures.

Consisting of disks (disk-type) brazed By post-mortem using microscopy for a CLIC prototype structure after its high-gradient test, microscopic gaps and suspicious objects were found around the diffusion bonded planes [12]. Brazing of disks might be a good solution, filling those gaps, although the accuracy is supposed to be lower than that by diffusion bonding. We have made a single-cell damped test cavity by brazing, where the test cell is based

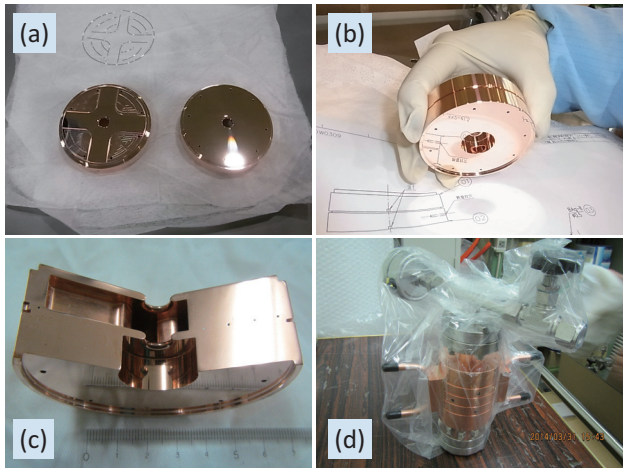

Figure 8: Test cavity with HOM waveguides, where disks were bonded by brazing. (a) Brazing filler metal and grooves. (b) Test brazing of two disks. (c) Checking the brazing performance. (d) Just after the delivery.

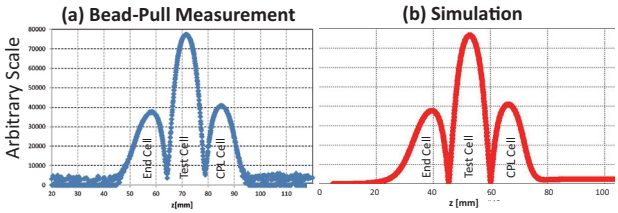

Figure 9: Comparison of the electric-field strength between the bead-pull measurement and simulation. CPL means coupling.

on TD24R05, as shown in Fig. 8. We have performed low-power RF measurements, and found no problem with no tuning. Figure 9 shows measured and simulated electric-field strengths along the beam axis, where the measurement is in good agreement with the simulation result.

Consisting of quadrants (quadrant-type) Quadrant-type structure has a definite advantage that no surface current associated with magnetic field flows across any junction or bonding plane [1] in addition to possible significant cost reduction by the simple machining and assembly [13]. We once fabricated a quadrant-type prototype structure with 18 cells, and performed a high-gradient test. The result was that the accelerating gradient was limited to 60 MV/m or lower, and we observed no conditioning effects [14]. Going back to its basics, we have identified disadvantages of the naive quadrant-type structure, and proposed measures to overcome all of the disadvantages, as shown in Fig. 10. Based on this new design, we have made quadrants of a single-cell structure for high-gradient testing [13]. After the machining of the quadrants by high-precision milling, we performed assembly in a highly-precise way as shown in Fig. 11.

[1] Typical surface current during X-band high-gradient tests is of the order of 10^8 A/cm^2.

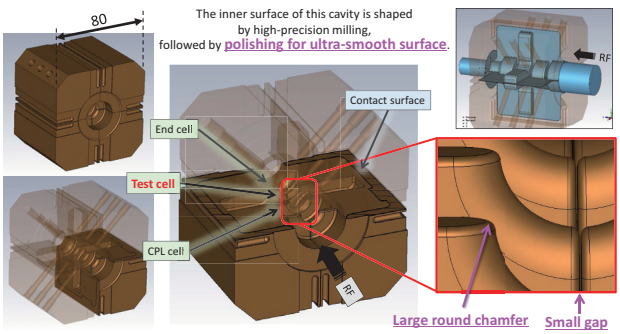

Figure 10: New quadrant-type structure as a single-cell test cavity, which overcomes all of the disadvantages. CPL means coupling.

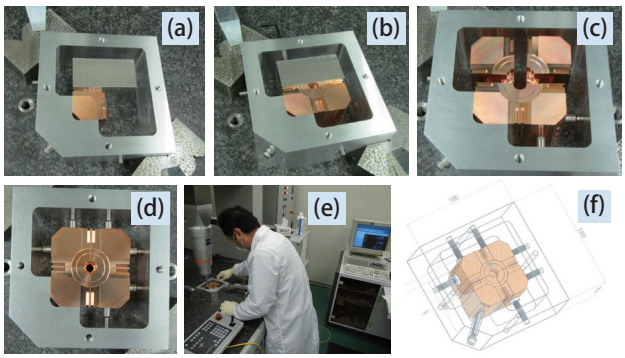

Figure 11: Precise assembly of the quadrants of the single-cell damped structure. (a) One quadrant fixed on an alignment frame. (b) Two quadrants aligned using an alignment block. (c) Replacing the alignment block by two quadrants. (d) After the last two quadrants aligned. (e) During the alignment of the last two quadrants using a CMM. (f) 3D drawing of the alignment frame including the quadrants.

After the precise assembly, we have performed electron beam welding (EBW) to bond the four quadrants with EBW conditions described in [13]. Bonding with EBW enables us to make accelerating structures made of hard copper only, leading possibly to lower BDR because of its higher tolerance for stress originated from the surface current [15]. Figure 12a is a photograph after the EBW. Figure 12b shows the welding penetration depth, which is 1.5 mm, and enough from mechanical and vacuum-sealing points of view. During the EBW, we measured temperature of one of the quadrants at a position shown in Fig. 12c, and found that maximum temperature rise measured at the position far from the EBW beads was lower than 10 degC. Finally, we have confirmed no vacuum leak with a background level lower than 1.0×10^{-10} Pa m^3/s.

We have measured the accelerating-mode frequency before and after the EBW by using a pickup antenna, and found that the frequency has become higher by 5.6 MHz. We have also measured transverse lengths by using a CMM before and after the EBW; the length change was -9.7 μm in average around the test cell, which corresponds to 7.2 MHz frequency increase if we assume uniform shrinkage only

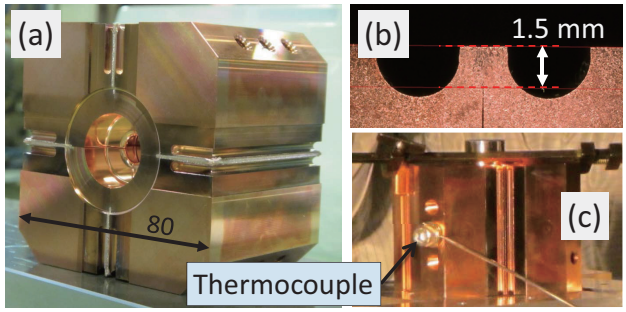

Figure 12: EBW of the quadrants. (a) After the EBW. (b) Welding penetration depth for the EBW conditions described in [13]. (c) A thermocouple is attached.

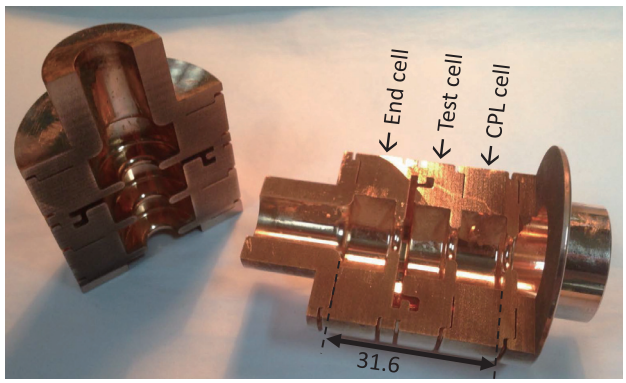

Figure 13: Photograph of the X-band single-cell test cavity with the choke-mode damped structure in the test cell. CPL means coupling. Courtesy of Tsinghua University.

at the contact surface of the adjacent quadrants during the EBW. Therefore, the measured frequency change of 5.6 MHz can be attributed to the transverse uniform shrinkage. It should be emphasized that such frequency change is within the scope of the frequency-tuning mechanism of this test cavity.

As for the surface finishing for quadrants, we have been testing an advanced polishing which meets the following requirements [16]:

- Ultra-smooth surface with $R_a < 10$ nm, and
- Applicability to any curved surface.

Choke-Mode Damped Structure

Choke-mode damped structure [17] is smart in its electrical design with axial symmetry and no enhancement of surface-magnetic field, and is successful at a C-band XFEL facility [18] although such structure is relatively complicated. Our collaborators at Tsinghua University (China) are working to make X-band accelerating structures with such choke-mode damped structure [19]. Figure 13 shows an X-band single-cell test cavity recently made by the team for bonding test and RF measurement. They are fabricating a corresponding test cavity for a high-gradient test to be performed at Shield-B.

SCHEDULE

The RF conditioning of the power line to Shield-B will be finished this summer. Then, we will replace the dummy load by a test cavity in Shield-B to check and establish the system of the monitoring and data acquisition. We will start the first high-gradient test for the standard cavity this coming autumn, including measurement of a "reference" BDR, where we will start a gradient range of 80 to 100 MV/m, which corresponds to practical applications. Then, we will step up the gradient, depending on results of the high-gradient test and our scientific interests. After the high-gradient test of the standard cavity, we will select and install a second test cavity from those shown in this paper.

SUMMARY

Basic study on vacuum breakdown, in the form of single cell, based on the X-band technology developed so far, is beginning at KEK / Nextef / Shield-B, where the klystron is working well, the RF conditioning of the power line is also progressing well, and the first high-gradient test will start this coming autumn.

We have many structures to be tested, including undamped and damped structures, structure with large grain, disks machined by turning only and by milling only, choke-mode structure, and new quadrants.

REFERENCES

[1] J. Wang and T. Higo, "Accelerator Structure Development for NLC/GLC," ICFA Beam Dynamics Newsletter **32**, 27, 2003.

[2] T. Higo *et al.*, "High Gradient Performance of TW Accelerator Structures Targeting 100 MV/m," in Proceedings of the 12th Annual Meeting of Particle Accelerator Society of Japan, August 2015 (Paper ID: WEP047).

[3] M. Aicheler *et al.*, "A Multi-TeV Linear Collider Based on CLIC Technology : CLIC Conceptual Design Report," CERN-2012-007, SLAC-R-985, KEK-Report-2012-1, PSI-12-01, JAI-2012-001.

[4] T. Higo *et al.*, "Advancement of High Gradient Study at 100 MV/m Range," in Proceedings of the 8th Annual Meeting of Particle Accelerator Society of Japan, August 2011 (Paper ID: TUPS129).

[5] T. Higo *et al.*, "Comparison of High Gradient Performance in Varying Cavity Geometries," in Proceedings of IPAC2013, Shanghai, China, 2013 (Paper ID: WEPFI018).

[6] V. A. Dolgashev, S. G. Tantawi, C. D. Nantista, Y. Higashi and T. Higo, "Travelling Wave and Standing Wave Single Cell High Gradient Tests," SLAC-PUB-10667, 2004.

[7] V. A. Dolgashev, S. G. Tantawi, Y. Higashi and T. Higo, "Status of High Power Tests of Normal Conducting Single-cell Structures," Conf. Proc. C **0806233**, MOPP083 (2008).

[8] C. Nantista, S. Tantawi and V. Dolgashev, "Low-Field Accelerator Structure Couplers and Design Techniques," Phys. Rev. ST Accel. Beams **7**, 072001 (2004).

[9] D. P. Pritzkau and R. H. Siemann, "Experimental study of RF pulsed heating on oxygen free electronic copper," Phys. Rev. ST Accel. Beams **5**, 112002 (2002).

[10] F. Wang, C. Adolphsen and C. Nantista, "Performance limiting effects in X-band accelerators," Phys. Rev. ST Accel. Beams **14**, 010401 (2011) [Phys. Rev. ST Accel. Beams **15**, 120402 (2012)].

[11] V. A. Dolgashev, J. Neilson, S. G. Tantawi and A. D. Yeremian, "A Dual-mode Accelerating Cavity to Test RF Breakdown Dependence on RF Magnetic Fields," Conf. Proc. C **110904**, 247 (2011).

[12] M. Aicherer, CERN EDMS, "SEM analysis," `http://indico.cern.ch/event/100482/`.

[13] T. Abe *et al.*, "Fabrication of Quadrant-Type X-Band Single-Cell Structure used for High Gradient Tests," in Proceedings of the 11th Annual Meeting of Particle Accelerator Society of Japan, August 2014 (Paper ID: SUP042).

[14] T. Higo, "KEK activities on CLIC X-band Accelerating Structures," presented at the mini-workshop on CLIC X-band structure R&D at THU, 2010 (`http://indico.cern.ch/event/89913/`).

[15] V. Dolgashev, S. Tantawi, A. Yeremian, Y. Higashi and B. Spataro, "Status of High Power Tests of Normal Conducting Single-Cell Standing Wave Structures," Conf. Proc. C **100523**, THPEA060 (2010).

[16] T. Abe, "Basic Study on High-Gradient Accelerating Structures at KEK / Nextef," presented at International Workshop on Breakdown Science and High Gradient Technology (HG2015), Tsinghua University, China, 2015 (`https://indico.cern.ch/event/358352/`).

[17] T. Shintake, "The Choke Mode Cavity," Jpn. J. Appl. Phys. 31, p.1567, 1992.

[18] T. Inagaki, C. Kondo, H. Maesaka, T. Ohshima, Y. Otake, T. Sakurai, K. Shirasawa and T. Shintake, "High-Gradient C-band Linac for a Compact X-ray Free-Electron Laser Facility," Phys. Rev. ST Accel. Beams **17**, no. 8, 080702 (2014).

[19] H. Zha, J. Shi, H. Chen, A. Grudiev, W. Wuensch, C. Tang and W. Huang, "Choke-Mode Damped Structure Design for the Compact Linear Collider Main Linac," Phys. Rev. ST Accel. Beams **15**, 122003 (2012).